Journal of Physics: Conference Series **318** (2011) 022028 doi:10.1088/1742-6596/318/2/022028

Effects of spatially varying slip length on friction drag reduction in wall turbulence

Yosuke Hasegawa[1,2], **Bettina Frohnapfel**[1] **& Nobuhide Kasagi**[2]

[1]Center of Smart Interfaces, TU Darmstadt, Germany,
[2]Department of Mechanical Engineering, The University of Tokyo, Japan

E-mail: hasegawa@thtlab.t.u-tokyo.ac.jp, frohnapfel@csi.tu-darmstadt.de, kasagi@thtlab.t.u-tokyo.ac.jp

Abstract. A series of direct numerical simulation has been made of turbulent flow over hydrophobic surfaces, which are characterized by streamwise periodic micro-grooves. By assuming that the size of micro-grooves is much smaller than the typical length-scale of near-wall turbulent structures, the dynamical boundary condition is expressed by a mobility tensor, which relates the slip velocity and the surface shear stress. Based on the derived mathematical relationship between the friction drag and different dynamical contributions, it is shown how the turbulence contribution can be extracted and analyzed.

1. Background

Previous studies have shown that a hydrophobic surface has considerable potential for friction drag reduction. In general, a hydrophobic slip effect can be achieved by fabricating nano- or micro-scale structured cavities on the surface. Small gas bubbles are trapped inside the cavities, over which a liquid flow experiences almost zero shear stress, while the no-slip condition holds at the top of the protrusion of the structured surface. When the Reynolds number is sufficiently small so that the flow remains laminar, analytical expressions for l over alternating slip and no-slip boundary conditions with different variational patterns have been obtained for the case of the Stokes limit by e.g., Philip (1972) and Lauga & Stone (2003).

Considering that most engineering flows are turbulent and that friction drag generally becomes larger there, application of a hydrophobic surface to turbulent flow is of great interest. Usually, the typical length-scale of the structured surface is much smaller than that of a flow, so that the velocity boundary condition over a hydrophobic surface is modeled as follows:

$$u_w = l\left(\frac{\partial u}{\partial y}\right)_w, \tag{1}$$

where l is the so-called slip length, which relates the slip velocity at the wall, u_w, with the wall-normal gradient of u_w at the wall (subscript w). Several numerical simulations by Min & Kim (2004) and Fukagata et al. (2006) show that, in turbulent flows, slip in the streamwise direction leads to a drag reduction effect similar to that in laminar flows, while slip in the spanwise direction causes increased friction drag due to modification of the near-wall turbulent structures. These studies imply that a hydrophobic surface would cause not only slip in the

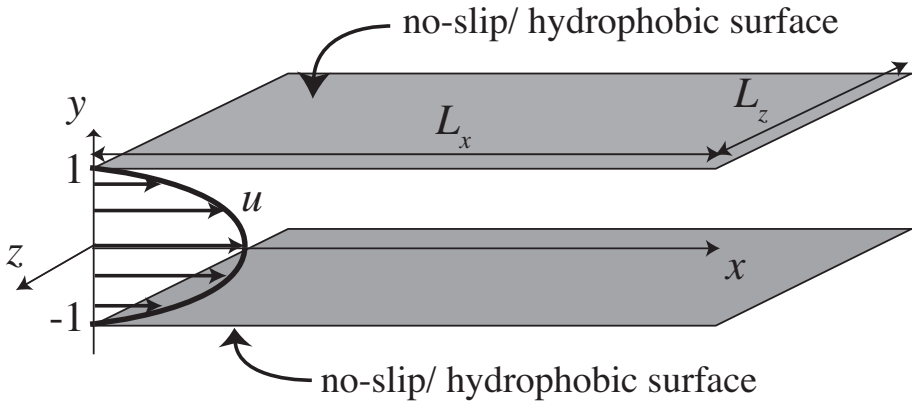

Figure 1. Computational domain and coordinate system

streamwise direction which directly results in drag reduction, but also modification of the turbulence dynamics providing a secondary effect on the skin friction drag. Although recent simulations study different geometric patterns of alternating slip and no-slip boundary conditions in turbulent flows (Martell et al. (2009)), their effect on the turbulence dynamics have not been investigated in detail.

In the present study, we systematically change the geometric pattern of no-slip and slip boundary conditions in order to investigate this effect on the turbulent skin friction drag. In order to quantify the two different contributions, which arise from the finite slip velocity and the modified turbulence, to the skin friction drag, we extend the so-called FIK identity (Fukagata et al. (2002)) to a hydrophobic surface. Through the present analysis, we aim at obtaining general knowledge on spatially varying slip patterns which diminish the turbulent friction drag.

2. Mathematical relationship between the bulk mean velocity and different dynamical contributions

2.1. No-slip surface

Fukagata et al. (2002) derived a general mathematical relationship between the skin friction coefficient, C_f, and different dynamical contributions in wall-bounded flows. Throughout this paper, the streamwise, wall-normal and spanwise coordinates are denoted as x, y and z, respectively, as shown in Fig. 1. The averaged streamwise momentum equation for a fully developed channel flow is given by:

$$0 = -\frac{\partial \overline{p}}{\partial x} + \frac{\partial}{\partial y}\left(\frac{1}{\mathrm{Re}}\frac{\partial \overline{u}}{\partial y} - \overline{u'v'}\right), \tag{2}$$

where all quantities are normalized by the bulk mean velocity U_b^* and the channel half depth δ^*. An asterisk denotes a dimensional quantity. A variable with an over-bar represents an averaged quantity in homogeneous directions, i.e., x, z and also time t, while a variable with a prime deviation from an averaged quantity. The Reynolds number is defined as $\mathrm{Re} = U_b^*\delta^*/\nu^*$. By applying triple integration to the above equation and taking into account no-slip conditions at top and bottom walls, the following identity can be obtained:

$$C_f = \frac{\tau_w^*}{\frac{1}{2}\rho^* U_b^{*2}} = \frac{6}{\mathrm{Re}} + 3\int_{-1}^{1} y\overline{u'v'}dy, \tag{3}$$

where ρ^* and τ_w^* are the fluid density and the wall shear stress, respectively. The first term on the right-hand-side corresponds to laminar drag and is constant once the flow rate is fixed, whereas the second term represents additional drag due to turbulence. The Reynolds shear stress $\overline{u'v'}$ which is weighted by y implies that the Reynolds stress near the wall contributes more to the skin friction drag than that in the central region of the channel.

2.2. Hydrophobic surface

When discussing the skin friction drag reduction, C_f is usually compared under a constant flow rate. However, this turns out to be not convenient to analyze a flow over a hydrophobic surface due to the presence of a slip velocity at the wall. A typical mean velocity profile between two parallel hydrophobic surfaces is illustrated in Fig 2. Due to a non-zero streamwise slip velocity $U_w = \overline{u_w}$, the total bulk mean velocity U_b is given by $U_b = U_w + U_r$, where we refer to U_r as the relative bulk mean velocity. From the viewpoint of turbulence dynamics, U_r (or the wall shear stress) plays an essential role. Hence, we consider a flow field under a constant pressure gradient instead of a constant flow rate, so as to keep the wall shear stress constant regardless of the boundary condition at the hydrophobic surface.

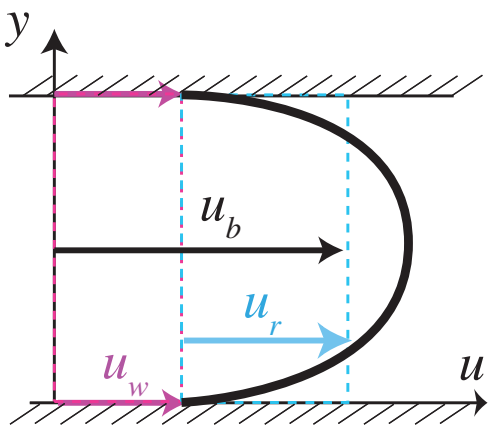

Figure 2. A conceptual mean velocity profile between two parallel hydrophobic surfaces.

When the mean pressure gradient is kept constant, the increase in mass flow rate is a measure for the effectiveness of a certain hydrophobic surface. The FIK identity (3) results in the following relationship between U_r and the weighted integral of the Reynolds shear stress:

$$U_r{}^+ = \frac{\mathrm{Re}_\tau}{3} - \frac{1}{2}\int_{-\mathrm{Re}_\tau}^{\mathrm{Re}_\tau} \frac{y^+}{\mathrm{Re}_\tau} \cdot \overline{u'^+ v'^+} dy^+. \tag{4}$$

Here, the friction Reynolds number is defined as $\mathrm{Re}_\tau = u_\tau^* \delta^* / \nu^*$, where u_τ^* is the friction velocity. The superscript $+$ denotes a quantity normalized by viscous wall units. The first term corresponds to the bulk mean velocity for the laminar flow over a no-slip surface, while the second term represents suppression of the bulk mean velocity due to turbulence. Consequently, the total bulk mean velocity $U_b{}^+$ can be represented as:

$$\begin{aligned} U_b{}^+ &= U_w{}^+ + U_r{}^+ \\ &= l_e^+ + \frac{\mathrm{Re}_\tau}{3} - \frac{1}{2}\int_{-\mathrm{Re}_\tau}^{\mathrm{Re}_\tau} \frac{y}{\mathrm{Re}_\tau} \cdot \overline{u'^+ v'^+} dy \end{aligned} \tag{5}$$

In deriving the above equation, we use the relationships of $U_w^+ = l_e^+(\partial\overline{u}^+/\partial y^+)_w$ and $(\partial u^+/\partial y^+)_w = 1$, where l_e^+ is the effective slip length. In a laminar flow, the third term, i.e., the turbulent contribution, is absent so that U_b can be enhanced only by increasing the slip length l_e^+. In a turbulent flow, however, the third term becomes dominant. Therefore, we expect an additional effect of hydrophobic surfaces on friction drag in turbulent flows.

3. Numerical Procedures

3.1. Numerical method

We consider a fully developed turbulent channel flow between two parallel plates as shown in Fig. 1. Periodic boundary conditions are imposed in the x and z directions. The governing equations for the velocity field are given by the Navier-Stokes and continuity equations:

$$\frac{\partial u_i}{\partial t} + \frac{\partial (u_j u_i)}{\partial x_j} = -\frac{\partial p}{\partial x_i} + \frac{1}{\mathrm{Re}} \frac{\partial u_i^2}{\partial x_j \partial x_j}, \tag{6}$$

$$\frac{\partial u_i}{\partial x_i} = 0. \tag{7}$$

Here, all quantities are normalized by the friction velocity u_τ^* and the channel half width δ^*.

As discussed in Sec. 1, a hydrophobic surface is characterized by alternating slip and no-slip surfaces caused by micro-scale structured cavities on the surface. Since resolving such small structures is quite expensive, the dynamical effect of a hydrophobic surface is modeled by introducing a generalized slip boundary condition. Such a strategy is valid, when the typical length-scale of surface structure is sufficiently smaller than that of the near-wall turbulence. Actually, the recent experimental results show that significant drag reduction is obtained when the roughness periodicity is less than five in wall units (Daniello et al. (2009)).

As for the surface-normal direction, a non-permeable condition is imposed so that

$$u_2 = 0 \ \ at \ \ y = 1 \text{ and } -1. \tag{8}$$

The slip boundary conditions along the wall can be generally expressed as:

$$u_{wi} = M_{ij} \tau_{wj}, \tag{9}$$

where $i, j = 1$ or 3 and M_{ij} is a mobility tensor, which relates the local tangential shear stress and the slip velocity. The mobility tensor for a given surface geometry is derived in Sec. 3.2.

3.2. Mobility tensor at a hydrophobic surface

In simple geometry, analytical solutions for Stokes flow exist. For periodic grooves parallel to the streamsiwe direction as shown in Fig. 3, the exact expression for the effective slip length l_e (Philip (1972)) is given by:

$$\frac{l_e}{L} = \frac{-1}{\pi} \log \left[\cos \left\{ \frac{\pi}{2} (1 - \phi_s) \right\} \right], \tag{10}$$

where $\phi_s = a/L$ is the solid fraction, while a and L are the width of solid-liquid interface and the roughness periodicity, respectively. In the limit of vanishing solid fraction, i.e., $\phi_s \to 0$, Eq. (10) is approximated by $l_e \sim L$ (Ybert et al. (2007)). In order for the present slip model to be valid, L should be smaller than the viscous layer thickness, and therefore l_e^+ should not exceed five approximately. It should be also noted that, in the case of periodic grooves perpendicular to the flow direction, the slip length reduces by half from the value given by Eq. (10) (Lauga & Stone (2003)).

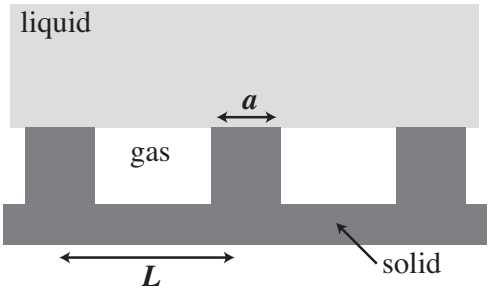

Figure 3. Schematic of a liquid phase over a hydrophobic wall.

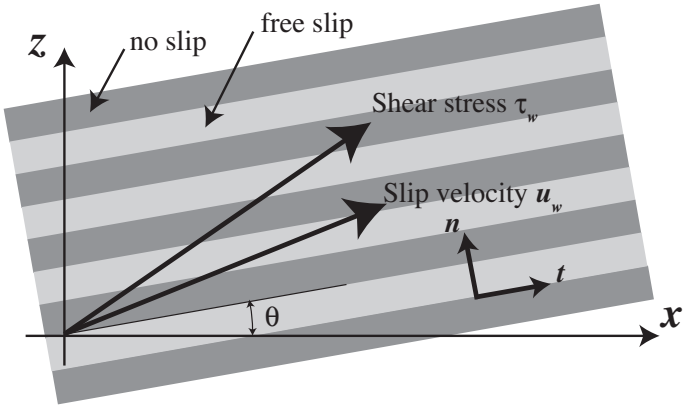

Figure 4. micro-grooved surface with an inclination angle θ with respect to the direction of a mean pressure gradient

If we consider micro-grooves tilted at a certain angle θ with respect to the direction of a mean pressure gradient (or free stream) as shown in Fig. 4, we can derive a relationship between the slip velocity u_w and the shear stress τ_w at a hydrophobic surface for an arbitrary value of θ.

The unit vector parallel to the micro-grooves is denoted t_j, while the normal vector n_j. They are respectively written as:

$$t_j = \begin{pmatrix} \cos\theta \\ \sin\theta \end{pmatrix}, \quad n_j = \begin{pmatrix} -\sin\theta \\ \cos\theta \end{pmatrix}. \tag{11}$$

We assume that the effective slip lengths in the directions of t_j and n_j are given by l_t and l_n, respectively. In addition, it is also assumed that the flow near the hydrophobic surface, i.e., within the viscous sublayer, can be approximated by a Stokes flow. This allows us to estimate the slip velocity by linear superposition of the shear stresses in the two orthogonal directions t_j and n_j as follows:

$$u_{wj} = l_t(\tau_{wi} \cdot t_i)t_j + l_n(\tau_{wi} \cdot n_i)n_j. \tag{12}$$

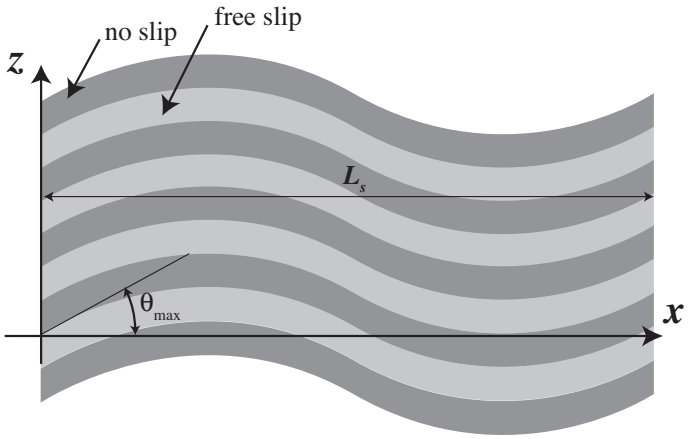

Figure 5. Schematic of a hydrophobic surface with the maximum inclination angle θ_{max} with respect to the direction of a mean pressure gradient

Substituting Eq. (11) into the above equation, we obtain:

$$\begin{aligned}
\begin{pmatrix} u_{w1} \\ u_{w3} \end{pmatrix} &= u_{wj} \\
&= l_t(\tau_{w1}\cos\theta + \tau_{w3}\sin\theta)\begin{pmatrix} \cos\theta \\ \sin\theta \end{pmatrix} \\
&+ l_n(-\tau_{w1}\sin\theta + \tau_{w3}\cos\theta)\begin{pmatrix} -\sin\theta \\ \cos\theta \end{pmatrix} \\
&= \begin{pmatrix} l_t\cos^2\theta + l_n\sin^2\theta & l_t\sin\theta\cos\theta - l_n\sin\theta\cos\theta \\ l_t\sin\theta\cos\theta - l_n\sin\theta\cos\theta & l_t\sin^2\theta + l_n\cos^2\theta \end{pmatrix}\begin{pmatrix} \tau_{w1} \\ \tau_{w3} \end{pmatrix} \qquad (13)
\end{aligned}$$

The above equation can be simplified to Eq. (9), where M_{ij} is the mobility tensor given by:

$$M_{ij} = \begin{pmatrix} l_t\cos^2\theta + l_n\sin^2\theta & l_t\sin\theta\cos\theta - l_n\sin\theta\cos\theta \\ l_t\sin\theta\cos\theta - l_n\sin\theta\cos\theta & l_t\sin^2\theta + l_n\cos^2\theta \end{pmatrix}, \qquad (14)$$

which relates the slip velocity and the shear stress at a hydrophobic surface.

3.3. Numerical scheme and test conditions

Equations (6)-(7) are solved by a pseudo-spectral method (essentially the same as that of Kasagi et al. (1992)), where Fourier expansion is employed in the x and z directions, while Chebyshev polynomials in the y direction. For time advancement, the second-order Adams-Bashforth and Crank-Nicolson methods are used for the convection and diffusion terms, respectively. All calculations are conducted under a constant pressure gradient with the friction Reynolds number of $\mathrm{Re}_\tau = u_\tau^*\delta^*/\nu^* = 150$. The computational domain size is $2.5\pi\delta$ and $\pi\delta$ in the x and z directions, respectively.

We consider a spatially varing pattern of micro-grooves as shown in Fig. 5. The geometric pattern is characterized by a single sinusoidal wave in the streamwise direction, while the width and depth of cavities are kept constant. Since the liquid in the vicinity of the hydrophobic surface tends to flow along the direction with the least resistance, i.e., parallel to the local micro-grooves, it is expected that such a geometry reproduces a spanwise slip velocity oscillating in the x direction, which might resemble the introduction of a spanwise wall velocity that is known

Table 1. Contributions from the different dynamical contributions in Eq. (5) to the bulk mean velocity

θ_{max}	no-slip	0	$\pi/8$	$2\pi/8$	$3\pi/8$	$4\pi/8$	$5\pi/8$	$6\pi/8$	$7\pi/8$
(1) l_e^+	0.0	5.0	4.9	4.7	4.5	4.1	3.7	3.3	2.9
(2) $\mathrm{Re}_\tau/3$	50.0	50.0	50.0	50.0	50.0	50.0	50.0	50.0	50.0
(3) $\int y\overline{u'v'}dy$	-34.9	-35.7	-35.8	-35.8	-35.8	-35.8	-36.1	-36.0	-36.4
(1)+(2)+(3)	15.3	19.3	19.1	19.0	18.6	18.3	17.6	17.3	16.5
U_b^+(DNS)	15.1	19.0	19.0	18.8	18.5	18.2	17.6	17.1	16.5

to cause significant drag reduction by suppressing near-wall turbulence (Viotti et al. (2009); Quadrio et al. (2009)). The steamwise oscillation period is set to be $L_s^+ = 1178$, which is close to a optimal wavelength reported in Viotti et al. (2009). The maximum angle θ_{max} of parallel grooves with respect to the flow direction is systematically changed as $\theta_{max} = (n/8)\pi$, where $n = 0-7$. Here, the case with $n = 0$ corresponds to the streamwise parallel grooves. The effective slip length in the tangential direction of the micro grooves is set to be $l_t^+ = 5$, whereas that in the normal direction is given by $l_n^+ = l_t^+/2 = 2.5$ in accordance with the analytical solution of the Stokes flow (Lauga & Stone (2003)). The generalized slip condition given by Eq. (8, 9) is implemented by taking into account the spatial change of θ in the streamwise direction.

4. Results

In Table 1, the contributions from the different dynamical effects in Eq. (5) to the bulk mean velocity are summarized. In all cases, the bulk mean velocity estimated by the sum of three terms on the right-hand-side of Eq. (5) agrees well with that obtained by DNS within deviation of 2%. This fact ensures that the flow fields reach fully developed states and validates the identity (5). We also note that the second term, i.e., the laminar contribution, is identical in all cases, since the friction Reynolds number is kept constant.

For a no-slip surface, only the second and third terms have non-zero values due to the absence of the surface slip. It is found that the third term, i.e. the turbulence contribution, has large magnitude, so that the resultant bulk mean velocity is significantly reduced from that for the laminar flow. This suggests a possibility of achieving significant increase of the bulk mean velocity by modifying turbulence. Compared with a no-slip surface, the bulk mean velocity over a hydrophobic surface with streamwise parallel grooves i.e., $\theta_{max} = 0$ is increased by $\Delta U_b^+ \simeq 4.0$. This increase in the bulk mean velocity is attributed to the changes in the first and second terms in Eq. (5). For the straight streamwise grooves, $l_e^+ = l_t^+ = 5.0$ according to Eq. (14), and this can be confirmed in Table 1. The third term of Eq. (5), i.e., the turbulent contribution, is found to be enhanced over a hydrophobic surface. For the straight grooves, the spanwise effect slip length is given by $l_n^+ = l_t^+/2 = 2.5$. It is known that the spanwise slip causes drag increase by enhancing near-wall vortical motions (Min & Kim (2004)). The enhancement of the turbulence contribution in the present study also agrees fairly well with the theoretical prediction by Fukagata et al. (2006).

For a hydrophobic surface with streamwise oscillating grooves, the first term, i.e., l_e^+, is gradually decreased with increasing θ_{max}. This is mainly because the spatial average of M_{11} in Eq. (14) is decreased with increasing θ_{max}. In contrast, the negative value of the third term, i.e., the turbulent contribution, is gradually enhanced with increasing θ_{max} and thus increasing spanwise slip length. In the present study, the suppression of turbulence due to the introduction of a spanwise wall velocity which sinusoidally varies in streamwise direction is not observed. Since both the first and third terms of Eq. (5) are decreased with increasing θ_{max}, the resultant

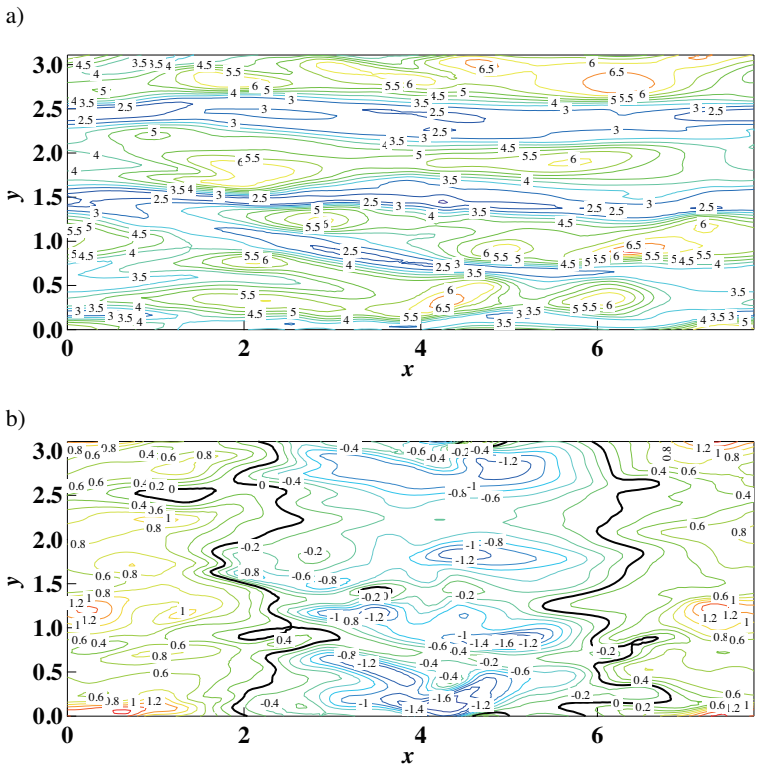

Figure 6. Instantaneous velocity at a hydrophobic surface with spatially oscillating micro-grooves at $\theta_{max} = 3\pi/8$. a) streamwise and b) spanwise velocity components

bulk mean velocity is monotonically decreased with increasing θ_{max}.

In Fig. 6, an instantaneous velocity field at a hydrophobic surface with streamwise oscillating micro-grooves at $\theta_{max} = 3\pi/8$ is shown. It is confirmed that a spanwise velocity oscillating in the streamwise direction is induced by the spatial pattern of micro-grooves. However, the typical amplitude of the spanwise slip velocity is about $w^+ = 1.0$ (see, Fig. 6 b), where the black lines represent $w^+ = 0$), and this is much smaller than that used in the previous studies (Viotti et al. (2009); Quadrio et al. (2009)). As a result, the near-wall streaks are hardly altered by the spanwise surface velocity as shown in Fig. 6 a). This would be a primary reason why the turbulent contribution term is not affected by the present hydrophobic surface. It should be also noted that the spanwise velocity at a hydrophobic surface is characterized by superposition of a spatially-periodic coherent component and a random fluctuation, while the spanwise wall velocity employed in the mentioned previous studies has only a coherent component. With increasing θ_{max}, M_{22} in Eq. (14) is increased, so that the effect spanwise slip becomes larger. Considering the fact that the spanwise slip contributes to drag increase, it is also possible that this compensates the drag reduction effect of the streamwise oscillating slip velocity.

5. Conclusions

In order to extract different dynamical contributions to turbulent skin friction at a hydrophobic surface, we extend the so-called FIK identity (Fukagata et al. (2002)) originally developed for a no-slip surface. By keeping the pressure gradient constant, a simple identity for the resultant bulk mean velocity is derived. The present identity indicates that the bulk mean velocity over a

hydrophobic surface is determined by three dynamical effects, i.e., the effective slip length, the laminar and turbulent contributions. In the present study, this identity is applied to hydrophobic surfaces with streamwise oscillating micro-grooves. It is found that the bulk mean velocity is increased mainly due to increase in the effective slip length, while the turbulent contribution is almost unchanged by the spatial pattern of micro-grooves. Further research will be carried out with the goal to indentify whether surface geometries for hydrophobic surfaces can be designed in such a way that they lead to significant suppression of the turbulence contribution to the skin friction drag.

References

Daniello, R. J., Waterhouse, N. E. & Rothstein, J. P. 2009 Drag reduction in turbulent flows over superhydrophobic surfaces *Phys. Fluids* **21**, 085103.

Fukagata, K., Iwamoto, K. & Kasagi, N. 2002 Contribution of Reynolds stress distribution to the skin friction in wall-bounded flows. *Phys. Fluids* **14**, L73–L76.

Fukagata, K., Kasagi, N. & Koumoutsakos, P. 2006 A theoretical prediction of friction drag reduction in turbulent flow by superhydrophobic surfaces. *Phys. Fluids* **18**, 051703.

Kasagi, N., Tomita, Y. & Kuroda, A. 1992 Direct numerical simulation of passive scalar field in a two dimensional turbulent channel flow. *Trans. ASME* J: *J. Heat Transfer* **114**, 598–606.

Lauga, E. & Stone, H.A. 2003 Effective slip in pressure-driven Stokes flow. *J. Fluid Mech.* **489**, 55–77.

Martell, M.B., Perot, J.B. & Rothstein, J.P. 2009 Direct numerical simulation of turbulent flow over ultrahydrophobic surfaces. *J. Fluid Mech.* **620**, 31–41.

Min, T. & Kim, J. 2004 Effects of hydrophobic surface on skin-friction drag. *Phys. Fluids* **15**, L55–L58.

Philip, J.R. 1972 Integral properties of flows satisfying mixed no-slip and no-shear conditions. *Z. Angew. Math. Phys.* **23**, 960–968.

Quadrio, M., Ricco, P. & Viotti, C. 2009 Streamwise-traveling waves of spanwise wall velocity in a turbulent channel flow. *J. Fluid Mech.* **627**, 161–178.

Viotti, C., Quadrio, M. & Luchini, P. 2009 Streamwise oscillations of spanwise wall velocity in a turbulent channel flow. *Phys. Fluids* **21**, 115109.

Ybert, C., Barentin, C., Cottin-Bizonne, C., Joseph, P. & Bocquet, L. 2007 Achieving large slip with superhydrophobic surfaces: Scaling laws for generic geometries. *Phys. Fluids* **19**, 123601.